

Isotope sensitive measurement of the hole-nuclear spin interaction in quantum dots

E. A. Chekhovich¹, M. M. Glazov², A. B. Krysa³, M. Hopkinson³,

P. Senellart⁴, A. Lemaître⁴, M. S. Skolnick¹, A. I. Tartakovskii¹

¹*Department of Physics and Astronomy, University of Sheffield, Sheffield S3 7RH, UK*

²*Ioffe Physical-Technical Institute of RAS, 194021 St. Petersburg, Russia*

³*Department of Electronic and Electrical Engineering,
University of Sheffield, Sheffield S1 3JD, UK*

⁴*Laboratoire de Photonique et de Nanostructures,
Route de Nozay, 91460 Marcoussis, France*

(Dated: November 2, 2018)

Decoherence caused by nuclear field fluctuations is a fundamental obstacle to the realization of quantum information processing using single electron spins^{1,2}. Alternative proposals have been made to use spin qubits based on valence band holes having weaker hyperfine coupling³⁻⁶. However, it was demonstrated recently both theoretically^{7,8} and experimentally⁹⁻¹¹ that the hole hyperfine interaction is not negligible, although a consistent picture of the mechanism controlling the magnitude of the hole-nuclear coupling is still lacking. Here we address this problem by performing isotope selective measurement of the valence band hyperfine coupling in InGaAs/GaAs, InP/GaInP and GaAs/AlGaAs quantum dots. Contrary to existing models^{7,8} we find that the hole hyperfine constant along the growth direction of the structure (normalized by the electron hyperfine constant) has opposite signs for different isotopes and ranges from -15% to $+15\%$. We attribute such changes in hole hyperfine constants to the competing positive contributions of p -symmetry atomic orbitals and the negative contributions of d -orbitals. Furthermore, we find that the d -symmetry contribution leads to a new mechanism for hole-nuclear spin flips which may play an important role in hole spin decoherence. In addition the measured hyperfine constants enable a fundamentally new approach for verification of the computed Bloch wavefunctions in the vicinity of nuclei in semiconductor nanostructures¹².

Due to the s -type character of the Bloch wavefunction, the hyperfine interaction of the conduction band electrons is isotropic (the Fermi contact interaction) and is described by a single hyperfine constant A , positive ($A > 0$) for most III-V semiconductors and proportional to the electron density at the nucleus. By contrast, for valence band holes the contact interaction vanishes due to the symmetry properties of the wavefunction, and the non-local dipole-dipole interaction dominates^{7,8,12-14}. As a result, the sign, magnitude and anisotropy of the hyperfine interaction depend on the actual form of the valence band Bloch wavefunction, which is usually not available with sufficient precision. Thus predicting the properties of the hole hyperfine coupling using first principle calculations remains a difficult task.

In this work we perform direct measurements of the hyperfine constants that describe the hole hyperfine interaction with nuclear spin along the growth axis of the structure (i.e. the diagonal elements of the hole hyperfine Hamiltonian). This is achieved by simultaneous and independent detection of the electron and hole Overhauser shifts using high resolution photoluminescence (PL) spectroscopy of neutral quantum dots. In contrast to previous work¹¹, we now also apply excitation with a radio-frequency (rf) oscillating magnetic field, which allows isotope-selective probing of

the valence band hole hyperfine interaction¹⁵. Using this technique we find that in all studied materials cations (gallium, indium) have negative hole hyperfine constant, while it is positive for anions (phosphorus, arsenic), a result attributed to the previously disregarded contribution of the cationic d -shells into the valence band Bloch wavefunctions.

Using the experimentally measured diagonal components of the hyperfine Hamiltonian (hole hyperfine constants) we calculate its non-diagonal part. We show that the admixture of the d -shells has a major effect on the symmetry of the hyperfine Hamiltonian: unlike pure p -symmetry heavy holes for which the hyperfine interaction has an Ising form⁸, the d -shell contribution results in non-zero non-diagonal elements of the hyperfine Hamiltonian. We predict this to be a major source of heavy hole spin decoherence.

Our experiments were performed on undoped GaAs/AlGaAs¹⁶, InP/GaInP¹¹ and InGaAs/GaAs¹⁵ QD samples without electric gates [further details can be found in the Supplementary Section S1]. PL of neutral QDs placed at $T = 4.2$ K, in external magnetic field B_z normal to the sample surface was measured using a double spectrometer and a CCD.

Our experiments rely on detection of PL of both "bright" and "dark" neutral excitons^{11,17-19} formed by electrons $\uparrow(\downarrow)$ with spin $\pm 1/2$ and heavy holes $\uparrow(\downarrow)$ with momentum $\pm 3/2$ parallel (antiparallel) to the growth axis Oz [see Fig. 1(a)]. Since the QDs contain on the order of 10^5 nuclei, non-zero average nuclear spin polarization of the k -th isotope $\langle I_z^k \rangle$ along the Oz axis can be treated as an additional magnetic field acting on the electron and hole spins. The coupling strength of the electron to the nuclear spins of isotope k is described by the hyperfine constant A^k . The additional energy of the exciton state with electron spin $\uparrow(\downarrow)$ is equal to $+\frac{1}{2}\Delta E_e^k$ ($-\frac{1}{2}\Delta E_e^k$), where the electron hyperfine shift induced by the k -th isotope is defined as

$$\Delta E_e^k = \rho^k A^k \langle I_z^k \rangle, \quad (1)$$

with ρ^k describing the relative concentration of the k -th isotope. For the heavy hole states the hyperfine interaction is described using a constant C^k expressed in terms of the normalized heavy-hole hyperfine constant γ^k as $C^k = \gamma^k A^k$. The variation of the energy of the exciton with hole spin $\uparrow(\downarrow)$ is $+\frac{1}{2}\Delta E_h^k$ ($-\frac{1}{2}\Delta E_h^k$), where the hole hyperfine shift is

$$\Delta E_h^k = \rho^k \gamma^k A^k \langle I_z^k \rangle \quad (2)$$

By taking the same values of ρ^k in Eqs. 1, 2 we assume for simplicity a uniform distribution of the average nuclear spin polarization and isotope concentration within the volume of the QD.

Detection of the hyperfine shifts is achieved using pump-probe techniques¹¹ [see timing diagram in Fig. 1 (b)]. The concept of the valence band hyperfine constant measurement is based on

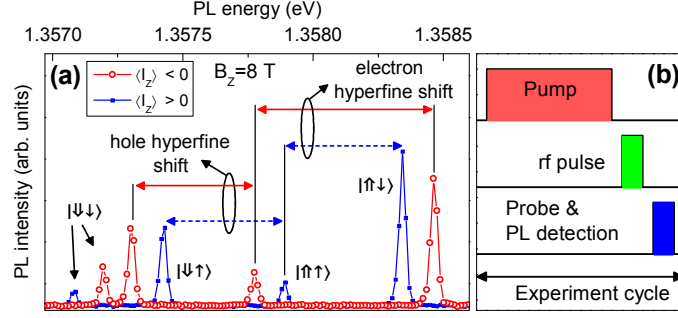


FIG. 1. (a) Photoluminescence spectra of a single neutral InGaAs/GaAs quantum dot in magnetic field $B_z \approx 8.0$ T. For low power optical excitation four PL lines are observed in each spectrum corresponding to all possible combinations of the electron spin states (\uparrow , \downarrow) and hole states (\uparrow , \downarrow) forming two bright excitons $|\uparrow\downarrow\rangle$, $|\downarrow\uparrow\rangle$ and two dark excitons $|\uparrow\uparrow\rangle$, $|\downarrow\downarrow\rangle$. In order to demonstrate independent detection of electron and hole hyperfine shifts two spectra are shown corresponding to negative (open symbols) and positive (solid symbols) nuclear spin polarization $\langle I_z \rangle$ induced on the dot by pumping with σ^+ and σ^- polarized light respectively. Strong change of the energy splitting between $|\uparrow\uparrow\rangle$ and $|\uparrow\downarrow\rangle$ excitons with opposite electron spin projections (see horizontal arrows) is equal to the electron hyperfine shift, while the much smaller change of the splitting between $|\uparrow\uparrow\rangle$ and $|\downarrow\uparrow\rangle$ states corresponds to the hole hyperfine shift. (b) Timing diagram of the pump-probe experiment used in the measurements of the hole hyperfine constants: Nuclear spin polarization is prepared with a long (~ 6 s) high power optical pump pulse. Following this, a radio-frequency oscillating magnetic field is switched on to achieve isotope selective depolarization of nuclear spins (rf pulse duration varies between 0.15 and 35 seconds depending on the material). Finally the sample is excited with a low power short (~ 0.3 s) probe laser pulse, during which the PL spectrum of both bright and dark excitons [similar to that in (a)] is measured. In all experiments the durations of the rf and probe pulses are much smaller than the natural decay time of the nuclear polarization. See further details of experimental techniques in Supplementary Sections S2, S3.

detecting ΔE_h^k as a function of ΔE_e^k by varying the nuclear spin polarization $\langle I_z^k \rangle$. Non-zero $\langle I_z^k \rangle$ is induced by optical nuclear spin pumping: circularly polarized light of the pump laser generates spin polarized electrons which transfer their polarization to nuclei^{15,17,20} via the hyperfine interaction (see details in Supplementary Section S2). The magnitude of $\langle I_z^k \rangle$ is controlled by changing the degree of circular polarization¹¹. According to Eqs. 1, 2 hole and electron hyperfine shifts depend linearly on each other ($\Delta E_h^k = \gamma^k \Delta E_e^k$) with slope equal to the normalized hole hyperfine constant γ^k . The electron (hole) hyperfine shift of a chosen (k -th) isotope is deduced from a differential measurement: the spectral splitting between excitons with opposite electron (hole) spins [see Fig. 1(a)] is measured (i) with an rf pulse which depolarizes only the k -th isotope and (ii) without any rf pulse. The difference between these two splittings is equal to ΔE_e^k (ΔE_h^k). Further details

of the isotope-selective experimental techniques are given in the captions of Figs. 1, 2 and in Supplementary Sections S2, S3.

We start by presenting results for unstrained GaAs/AlGaAs QDs. Optically detected nuclear magnetic resonance is well studied for these structures^{16,20}. A typical NMR spectrum consists of well resolved narrow peaks corresponding to three isotopes: ⁷⁵As, ⁶⁹Ga, ⁷¹Ga. Thus independent depolarization of a selected isotope is straightforward and is achieved by applying an oscillating rf field at the corresponding resonant frequency (see Supplementary Section S3 for further details).

The dependence of ΔE_h^k on ΔE_e^k for $k = ^{75}\text{As}$ is shown in Fig. 2 (a) for GaAs QD A1 (squares). Similar measurements are carried out for gallium nuclei. For that we take into account that both ⁶⁹Ga and ⁷¹Ga isotopes have nearly equal chemical properties resulting in equal values of the relative hole hyperfine interaction constants $\gamma^{^{69}\text{Ga}} = \gamma^{^{71}\text{Ga}} = \gamma^{Ga}$. Thus measurement of γ^{Ga} can be accomplished by erasing both ⁶⁹Ga and ⁷¹Ga polarization (which improves the measurement accuracy). The result of this experiment for the same QD is shown in Fig. 2 (a) (circles). It can be seen that the dependences for both Ga and As are linear as predicted by Eqs. 1, 2. Fitting gives the following values for the hole hyperfine constants $\gamma^{Ga} = -7.0 \pm 4.0\%$ and $\gamma^{As} = +15.0 \pm 4.5\%$. Similar measurements were performed on three other GaAs QDs. The resulting values are given in Table I. Since the variation between different dots is within experimental error, we take average values for all dots yielding $\gamma^{Ga} = -7.5 \pm 3.0\%$ and $\gamma^{As} = +16.0 \pm 3.5\%$. We thus conclude that different isotopes have opposite signs of the hole hyperfine constants: they are positive for arsenic and negative for gallium. This is an unexpected result in comparison with previous theoretical studies^{7,8} and experiments insensitive to individual isotopes where negative values of γ have been found in InP and InGaAs QDs^{10,11}.

We have also performed isotope-sensitive measurements of the hole nuclear interaction in InGaAs/GaAs QDs. These QDs have a more complicated nuclear spin system, due to significant strain-induced quadrupole effects^{15,21}. However, the isotope selective techniques used for GaAs/AlGaAs QDs are still applicable except that ¹¹⁵In and ⁶⁹Ga NMR spectra overlap, so that their nuclear spin polarizations can only be erased simultaneously.

The dependence of ΔE_h^k on ΔE_e^k for InGaAs QD B1 is shown in Fig. 2 (b) for ⁷¹Ga (circles), ⁷⁵As (squares) and for the total hyperfine shifts of ⁶⁹Ga and ¹¹⁵In (triangles). The hyperfine constant of indium can be determined if we use the hyperfine shift measured on ⁷¹Ga to separate the contributions of ¹¹⁵In and ⁶⁹Ga (see details in Supplementary Section S3B). The measured values of γ^k are summarized in Table I. Similar to GaAs, we find that arsenic has a positive hole hyperfine constant while for gallium and indium it is negative.

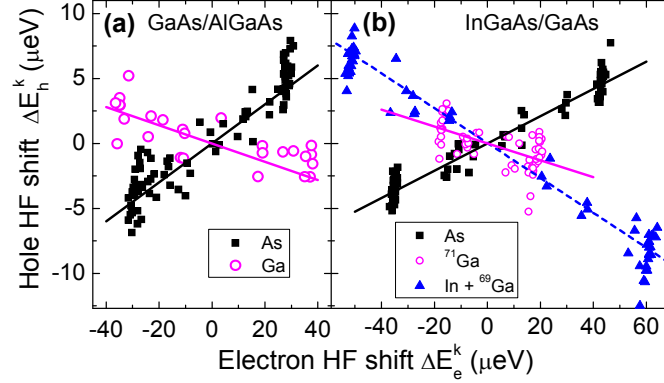


FIG. 2. Dependence of the hole hyperfine shift ΔE_h^k on the electron hyperfine shift ΔE_e^k for different isotopes in GaAs QD A1 (a) and InGaAs QD B1 (b). Nuclear spin polarization degree on the dot is varied by changing the degree of circular polarization of the pump laser pulse. The resulting electron hyperfine shift for isotope k is found as the difference of the energy splitting ($E_{\uparrow\uparrow} - E_{\uparrow\downarrow}$) of the $\uparrow\uparrow$ and $\uparrow\downarrow$ excitons measured without rf-excitation and the splitting ($E_{\uparrow\uparrow}^k - E_{\uparrow\downarrow}^k$) of the same excitons but measured after erasure of the nuclear polarization corresponding to the k -th isotope by the rf pulse. In the same way, the hole hyperfine shift is measured as $\Delta E_h^k = (E_{\uparrow\uparrow} - E_{\downarrow\uparrow}) - (E_{\uparrow\uparrow}^k - E_{\downarrow\uparrow}^k)$. Solid lines show fitting: the slopes correspond to the relative hole-nuclear hyperfine constants γ^k . We find $\gamma^{Ga} \approx -7.0\%$, $\gamma^{As} \approx +15.0\%$ for GaAs QD A1 and $\gamma^{Ga} \approx -6.5\%$, $\gamma^{As} \approx +10.5\%$ for InGaAs QD B1. Since the NMR resonances of ^{69}Ga and ^{115}In in InGaAs cannot be resolved, we measure the total hyperfine shifts $\Delta E_e^{In+^{69}Ga}$ and $\Delta E_h^{In+^{69}Ga}$ produced by these isotopes. Further analysis gives $\gamma^{In} \approx -16.0\%$ for QD B1 (see Supplementary Section S3B). Dashed line in (b) is a guide to the eye.

Applying the isotope selection techniques to InP/GaInP quantum dots studied previously¹¹ we find $\gamma^{In} = -12.5 \pm 3.0\%$ consistent with our previous results obtained without isotope selection¹¹. Similar to GaAs and InGaAs QDs we find a large positive constant for anions (phosphorus) $\gamma^P = +18.0 \pm 8.0\%$.

The values of γ presented in Table I describe hyperfine interaction of the valence band states that are in general mixed states of heavy and light holes. However as we show in detail in Supplementary Section S5 such mixing can not account for the opposite signs of γ^k observed for the cations and anions, but might be the reason for the dot-to-dot variation of γ^{In} observed in InP QDs (see Table I).

From the measurements without rf-pulses (similar to earlier isotope nonselective experiments of Refs.^{10,11}) we find that in GaAs QDs the total hole hyperfine shift (induced by all isotopes) is positive and amounts to $\gamma \approx +5\%$ relative to the total electron hyperfine shift. For the studied InGaAs QDs where indium and gallium concentrations are estimated to be $\rho^{In} \approx 20\%$ and $\rho^{Ga} \approx$

80% (see Ref.¹⁵) we find negative $\gamma \approx -4\%$, while for more indium rich InGaAs dots emitting at $E_{PL} \sim 1.30$ eV the value of $\gamma \approx -9\%$ has been reported¹⁰. This suggests that for QDs with a particular indium concentration ($\rho^{In} \sim 10\%$) one can expect close to zero ($\gamma \approx 0$) total hole hyperfine shift induced by nuclear spin polarization along Oz direction. Hole spin qubits in such structures will be insensitive to static nuclear fields which are induced by the optical control pulses and cause angle errors in spin rotations. Such spin qubits will benefit from a simplified implementation of the coherent control protocols⁶.

We now turn to analysis of the experimental results presented in Table I. First-principle calculation of the valence band hyperfine coupling requires integration of the hyperfine Hamiltonian using explicit expressions for the Bloch wavefunctions. Each nucleus is coupled to a hole which

TABLE I. Experimentally measured photoluminescence energies E_{PL} and hole hyperfine constants γ^k for different isotopes k in several GaAs and InGaAs QDs. Error estimates give 90% confidence values. Average values for each isotope in each material are given at the bottom of the table.

Material/QD	$\gamma^{Ga}, \%$	$\gamma^{In}, \%$	$\gamma^{As}, \%$	$\gamma^P, \%$	E_{PL}, eV
GaAs/AlGaAs:					
QD A1	-7.0±4.0	-	+15.0±4.5	-	1.713
QD A2	-8.5±3.5	-	+17.0±5.0	-	1.713
QD A3	-5.5±4.5	-	+15.0±4.0	-	1.702
QD A4	-7.5±4.5	-	+18.5±5.5	-	1.707
InGaAs/GaAs:					
QD B1	-6.5±5.5	-16.0±4.0	+10.5±2.0	-	1.358
QD B2	-3.0±6.5	-15.5±5.0	+10.0±3.0	-	1.358
QD B3	-5.5±5.0	-16.0±4.0	+8.0±2.0	-	1.357
QD B4	-4.5±7.0	-13.0±4.5	+8.5±3.0	-	1.357
InP/GaInP:					
QD C1	-	-15.5±1.5	-	+17.5±11.0	1.834
QD C2	-	-15.0±1.5	-	+18.5±12.5	1.851
QD C3	-	-9.0±1.5	-	+19.0±12.0	1.844
QD C4	-	-10.5±1.5	-	+17.5±11.0	1.834
Average:					
InGaAs/GaAs	-5.0±4.5	-15.0±3.5	+9.0±2.0	-	
GaAs/AlGaAs	-7.5±3.0	-	+16.0±3.5	-	
InP/GaInP	-	-12.5±3.0	-	+18.0±8.0	

spreads over many unit cells. However, it has been shown that the main effect arises from the short-range part of the dipole-dipole interaction^{8,14} (i.e. coupling of the nuclear spin with the wavefunction within the same unit cell). This allows a simplified approach to be used: the Bloch functions of the valence band maximum (corresponding to heavy-hole states) can be taken in the form $(-1/\sqrt{2})(\mathcal{X}(\vec{r}) + i\mathcal{Y}(\vec{r}))|\uparrow\rangle$ and $(1/\sqrt{2})(\mathcal{X}(\vec{r}) - i\mathcal{Y}(\vec{r}))|\downarrow\rangle$, where $|\uparrow\rangle, |\downarrow\rangle$ are spinors with corresponding spin projections on the Oz axis and $\mathcal{X}(\vec{r}) = X(\theta, \phi)R(r)$, $\mathcal{Y}(\vec{r}) = Y(\theta, \phi)R(r)$ are orbitals that transform according to the F_2 representation of the T_d point group relevant to bulk zinc-blende crystals (such as GaAs). Here the $\mathcal{X}(\vec{r})$ and $\mathcal{Y}(\vec{r})$ orbitals are decomposed into a real radial part $R(r)$ and angular parts $X(\theta, \phi)$, $Y(\theta, \phi)$. As a first approximation the angular parts of the orbitals can be taken in the form $X_p \propto x/r$, $Y_p \propto y/r$ (corresponding to p -type states with orbital momentum $l = 1$), while $R_p(r)$ can be approximated by hydrogenic radial functions. Calculations based on these functions^{7,8,14} yield positive hole hyperfine constant $\gamma^k > 0$ for all isotopes, in contradiction with our experimental findings (further details may be found in Supplementary Section S4).

This disagreement can be overcome by taking into account the contribution of shells with higher orbital momenta l , resulting in more accurate approximation of the hole wavefunction²². In particular we consider the contribution of the d -shell states ($l = 2$) that transform according to the F_2 representation of the T_d point group²³. We assume that the heavy-hole orbitals can be taken as normalized linear combinations of the form $\mathcal{X}(\vec{r}) = \alpha_p X_p(\theta, \phi)R_p(r) + \alpha_d X_d(\theta, \phi)R_d(r)$ where α_l are weighting coefficients ($|\alpha_p|^2 + |\alpha_d|^2 = 1$) and all orbitals X_l corresponding to orbital momentum l transform according to the same F_2 representation [d -shell states have the form $X_d \propto yz/r^2$, $Y_d \propto xz/r^2$, both p and d orbitals are schematically depicted in Fig. 3(a)]. Calculation of the relative hole hyperfine constant yields:

$$\begin{aligned} \gamma^k &= \frac{12}{5}|\alpha_p|^2 M_p - \frac{18}{7}|\alpha_d|^2 M_d, \\ M_l &= \frac{1}{|S(0)|^2} \int_0^\infty \frac{R_l^2(r)}{r} dr, \end{aligned} \quad (3)$$

where positive integrals M_l ($l = p, d$) depend on the radial wavefunctions $R_l(r)$ normalized by the density $(4\pi)^{-1}|S(0)|^2$ of the conduction band electron wavefunction at the nuclear site (see further information in Supplementary Section S4).

It follows from Eq. 3 that unlike the p -shell, the d -shell gives rise to a *negative* contribution to γ^k : importantly the sign of the hyperfine interaction is totally determined by the angular symmetry of the wavefunction, while the radial part only affects the magnitude of the contribution. We note that any hybridization of the valence band states with s orbitals due to QD symmetry reduction

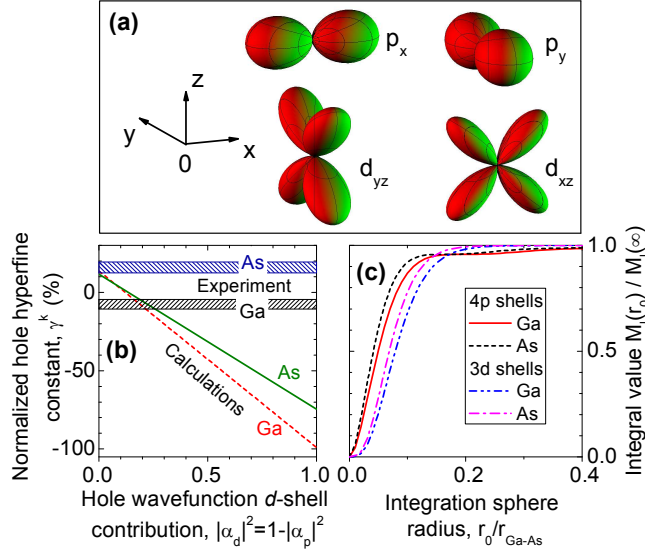


FIG. 3. (a) Schematic representations of p and d orbitals that transform according to the F_2 representation of the T_d point group. (b) Calculated dependence of the relative hole hyperfine constant γ^k of Ga and As as a function of d -shell contribution $|\alpha_d|^2$ (lines). Horizontal bands show experimentally measured confidence intervals for γ^k for GaAs QDs (see Table I). (c) Dependence of integrals $M_l(r_0)$ (see Eq. 3) on the upper integration limit r_0 for $3d$ and $4p$ shells for both Ga and As. Values of $M_l(r_0)$ are normalized by their values at $r_0 \rightarrow \infty$, while r_0 is normalized by the distance between Ga and As nuclei $r_{Ga-As} \approx 0.245$ nm in GaAs. The rapid saturation of the $M_l(r_0)$ variations shows that the major contribution to the hole hyperfine interaction ($>95\%$) arises from a small volume with a radius of $r_0 \lesssim 0.15 \times r_{Ga-As}$ around the nucleus.

would lead to a positive contribution to γ^k and thus can not account for the negative hyperfine constants⁸. In order to obtain numerical estimates we consider GaAs material and approximate $S(r)$, $R_p(r)$, $R_d(r)$ with radial hydrogenic wavefunctions corresponding to $4s$, $4p$ and $3d$ shells, respectively, taken with effective orbital radii^{8,24}. The resulting calculated dependence of γ^k on d -shell admixture $|\alpha_d|^2$ is shown in Fig. 3 (b) for $k = \text{Ga}$ and $k = \text{As}$ nuclei. Comparing with the experimental results of Table I [shown by the horizontal bands in Fig. 3 (b)] we conclude that the symmetry of the wavefunction on the anions (arsenic) is close to pure p -type, whereas for the cation gallium a significant contribution of the d -shell ($\sim 20\%$) is required to account for the negative hole hyperfine constant measured experimentally.

The non-zero contribution of the d -symmetry orbitals has a further unexpected effect on the hole hyperfine interaction: we find (see Supplementary Section S5) that the hyperfine interaction induces spin flips between the heavy hole states \uparrow and \downarrow . This is in contrast to the case of pure p -symmetry heavy hole states for which the hyperfine interaction has an Ising form⁸: in that case the symmetry of the system is artificially raised to spherical, resulting in hyperfine interaction

conserving angular momenta. The inclusion of the d -shells reduces the symmetry of the system down to that of the real crystal (described by the T_d point group). Under these conditions the hyperfine interaction does not conserve angular momentum and has non-zero non-diagonal elements coupling heavy holes with the opposite spins.

It was demonstrated previously that heavy-light hole mixing can result in a non-Ising form of the hyperfine interaction^{7,8}. However, our estimates show that for gallium in GaAs the contribution of the d -shells to the non-diagonal matrix elements of the hyperfine Hamiltonian dominates over the effect of the heavy-light hole mixing even if the valence band states have light hole contribution as large as $\sim 30\%$ (see Supplementary Section S5). A similar effect is expected for the other studied materials, since for all of them significant contribution of the cation d -shells is observed (resulting in $\gamma^k < 0$). Thus the d -orbital contribution will be a source of heavy hole spin dephasing even in the absence of mixing with light holes and should be taken into account when analyzing experimentally measured hole spin coherence times.

The hyperfine interaction is particularly strong in the small volume around the atomic core¹². To estimate this volume we limit the integration in Eq. 3 to a sphere of a radius r_0 , which makes M_l (and hence γ^k) a function of r_0 . The dependence of $M_l(r_0/r_{Ga-As})$ on the radius of the integration sphere, normalized by the distance between nearest Ga and As neighbors $r_{Ga-As} \approx 0.245$ nm, is shown in Fig. 3(c) for $3d$ and $4p$ shells for both Ga and As [since $M_l(r_0 \rightarrow \infty)$ converges it is normalized by its limiting value $M_l(\infty)$]. It can be seen that the main contribution to the integral ($>95\%$) comes from the small volume within a sphere with a radius of $\sim 0.15 \times r_{Ga-As}$, while the outer volume gives only a minor contribution due to the rapid decrease of the dipole-dipole interaction strength with increasing distance. Thus hyperfine coupling can be used to probe the structure of the wavefunction in the atomic core.

Our results on Bloch wavefunction orbital composition are in general agreement with existing theoretical models: the importance of d -shells in describing the valence band states is well recognized^{22,25}, and it has been shown that the d -symmetry contribution originates mainly from cations. However, the previous reports^{23,26,27} predicted much larger d -symmetry contribution ($|\alpha_d|^2$ exceeding 50%) than estimated in our work ($|\alpha_d|^2 \sim 20\%$). Such deviation might be due to the simplified character of our calculations and/or due to the intrinsic limitations of the wavefunction modeling techniques such as tight-binding or pseudo-potential methods²⁸ that fail to reproduce the wavefunction structure in the vicinity of the nucleus.

Theoretical modeling of the microscopic wavefunctions allows band structures to be calculated and thus is of importance both for fundamental studies and technological applications of

semiconductors²⁸. However, since true first-principle calculation of the many-body wavefunction is highly challenging, empirical approaches are normally used. They ultimately rely on fitting model parameters to describe the set of experimental data (e.g. energy gaps, effective masses, X-ray photoemission spectra). The experimental data on the valence band hyperfine parameters obtained in this work provides a means for probing the hole Bloch wavefunction: it allows direct analysis of the wavefunction orbital composition in the close vicinity of the nuclei, where theoretical modeling is the most difficult. Furthermore our experimental method is unique in being isotope-selective thus allowing independent study of cation and anion wavefunctions. The techniques developed in this work for quantum dots have the potential to be extended to other semiconductor systems, e.g. bound excitons in III-V and group-IV bulk semiconductors where dark excitons are observed²⁹ and hyperfine shifts can be induced and detected³⁰.

A rigorous modeling of the hyperfine parameters¹² has not been carried out so far for the valence bands states of III-V semiconductor nanostructures. Progress in this direction will provide a better understanding of the mechanisms controlling the sign and magnitude of the valence-band hyperfine coupling. In particular the potential effect of large inhomogeneous elastic strain (present in self-assembled quantum dots) on the microscopic Bloch hole wavefunction needs to be examined. This may be a possible route to engineering of holes with reduced hyperfine coupling.

ACKNOWLEDGMENTS The authors are thankful to M. Nestoklon, A. J. Ramsay, D. N. Krizhanovskii and M. Potemski for fruitful discussion and to D. Martrou for help with the GaAs sample growth. This work has been supported by EPSRC Programme Grant No. EP/G001642/1, the Royal Society, and ITN Spin-Optronics. M.M.G. was supported by the RFBR, RF President Grant NSh-5442.2012.2 and EU project SPANGL4Q.

AUTHOR CONTRIBUTIONS A.B.K., M.H., P.S. and A.L. developed and grew the samples. E.A.C. and A.I.T. conceived the experiments. E.A.C. developed the techniques and carried out the experiments. E.A.C., M.M.G. and A.I.T. analyzed the data. E.A.C., M.M.G., A.I.T. and M.S.S. wrote the manuscript with input from all authors.

ADDITIONAL INFORMATION Correspondence and requests for materials should be addressed to E.A.C. (e.chekhovich@sheffield.ac.uk) and A.I.T. (a.tartakovskii@sheffield.ac.uk)

¹ Khaetskii, A. V., Loss, D., and Glazman, L. Electron spin decoherence in quantum dots due to interaction with nuclei. *Phys. Rev. Lett.* **88**, 186802 (2002).

- ² Bluhm, H. *et al.* Dephasing time of GaAs electron-spin qubits coupled to a nuclear bath exceeding 200 us. *Nature Phys.* **7**, 109–113 (2011).
- ³ Brunner, D. *et al.* A coherent single-hole spin in a semiconductor. *Science* **325**, 70–72 (2009).
- ⁴ Heiss, D. *et al.* Observation of extremely slow hole spin relaxation in self-assembled quantum dots. *Phys. Rev. B* **76**, 241306 (2007).
- ⁵ Grelich, A., Carter, S. G., Kim, D., Bracker, A. S., and Gammon, D. Optical control of one and two hole spins in interacting quantum dots. *Nature Photon.* **5**, 702 (2011).
- ⁶ De Greve, K. *et al.* Ultrafast coherent control and suppressed nuclear feedback of a single quantum dot hole qubit. *Nature Phys.* **7**, 872–878 (2011).
- ⁷ Testelin, C., Bernardot, F., Eble, B., and Chamarro, M. Hole–spin dephasing time associated with hyperfine interaction in quantum dots. *Phys. Rev. B* **79**, 195440 (2009).
- ⁸ Fischer, J., Coish, W. A., Bulaev, D. V., and Loss, D. Spin decoherence of a heavy hole coupled to nuclear spins in a quantum dot. *Phys. Rev. B* **78**, 155329 (2008).
- ⁹ Eble, B. *et al.* Hole-nuclear spin interaction in quantum dots. *Phys. Rev. Lett.* **102**, 146601 (2009).
- ¹⁰ Fallahi, P., Yilmaz, S. T., and Imamoglu, A. Measurement of a heavy-hole hyperfine interaction in InGaAs quantum dots using resonance fluorescence. *Phys. Rev. Lett.* **105**, 257402 (2010).
- ¹¹ Chekhovich, E. A., Krysa, A. B., Skolnick, M. S., and Tartakovskii, A. I. Direct measurement of the hole-nuclear spin interaction in single InP/GaInP quantum dots using photoluminescence spectroscopy. *Phys. Rev. Lett.* **106**, 027402 (2011).
- ¹² Van de Walle, C. G. and Blöchl, P. E. First-principles calculations of hyperfine parameters. *Phys. Rev. B* **47**, 4244–4255 (1993).
- ¹³ Abragam, A. *The principles of Nuclear Magnetism*. Oxford University Press, London (1961).
- ¹⁴ Gryncharova, E. I. and Perel, V. I. Relaxation of nuclear spins interacting with holes in semiconductors. *Sov. Phys. Semicond.* **11**, 997 (1977).
- ¹⁵ Chekhovich, E. A., *et al.* Structural analysis of strained quantum dots using nuclear magnetic resonance. *Nature Nanotech.* DOI:10.1038/NNANO.2012.142 (2012).
- ¹⁶ Makhonin, M. N. *et al.* Fast control of nuclear spin polarization in an optically pumped single quantum dot. *Nature Materials* **10**, 844–848 (2011).
- ¹⁷ Chekhovich, E. A., Krysa, A. B., Skolnick, M. S., and Tartakovskii, A. I. Light-polarization-independent nuclear spin alignment in a quantum dot. *Phys. Rev. B* **83**, 125318 (2011).
- ¹⁸ Bayer, M. *et al.* Fine structure of neutral and charged excitons in self-assembled In(Ga)As/(Al)GaAs quantum dots. *Phys. Rev. B* **65**, 195315 (2002).
- ¹⁹ Poem, E. *et al.* Accessing the dark exciton with light. *Nature Phys.* **6**, 993–997 (2010).
- ²⁰ Gammon, D. *et al.* Nuclear Spectroscopy in Single Quantum Dots: Nanoscopic Raman Scattering and Nuclear Magnetic Resonance. *Science* **277**, 85–88 (1997).
- ²¹ Flisinski, K. *et al.* Optically detected magnetic resonance at the quadrupole-split nuclear states in (In,Ga)As/GaAs quantum dots. *Phys. Rev. B* **82**, 081308 (2010).

- ²² Jancu, J.-M., Scholz, R., Beltram, F., and Bassani, F. Empirical spds* tight-binding calculation for cubic semiconductors: General method and material parameters. *Phys. Rev. B* **57**, 6493–6507 (1998).
- ²³ Boguslawski, P. and Gorczyca, I. Atomic-orbital interpretation of electronic structure of III-V semiconductors: GaAs versus AlAs. *Semiconductor Science and Technology* **9**, 2169 (1994).
- ²⁴ Clementi, E. and Raimondi, D. L. Atomic screening constants from scf functions. *The Journal of Chemical Physics* **38**, 2686–2689 (1963).
- ²⁵ Persson, C. and Zunger, A. $s - d$ coupling in zinc-blende semiconductors. *Phys. Rev. B* **68**, 073205 (2003).
- ²⁶ Chadi, D. Angular momentum decomposition of $k = 0$ Bloch functions in group IV and zincblende crystals. *Solid State Communications* **20**, 361 – 364 (1976).
- ²⁷ Díaz, J. G. and Bryant, G. W. Electronic and optical fine structure of GaAs nanocrystals: The role of d orbitals in a tight-binding approach. *Phys. Rev. B* **73**, 075329 (2006).
- ²⁸ Di Carlo, A. Microscopic theory of nanostructured semiconductor devices: beyond the envelope-function approximation. *Semiconductor Science and Technology* **18**, R1 (2003).
- ²⁹ Merz, J. L., Faulkner, R. A., and Dean, P. J. Excitonic molecule bound to the isoelectronic nitrogen trap in GaP. *Phys. Rev.* **188**, 1228–1239 (1969).
- ³⁰ Steger, M. *et al.* Quantum information storage for over 180 s using donor spins in a ^{28}Si semiconductor vacuum. *Science* **336**, 1280–1283 (2012) and references therein.

SUPPLEMENTARY INFORMATION

The document consists of the following sections:

- S1. Details of sample structure and growth,
- S2. Details of experimental techniques,
- S3. Isotope selective depolarization of nuclear spins,
- S4. Calculation of the valence band hyperfine interaction strength,
- S5. Hole hyperfine interaction in quantum dots.

S1. DETAILS OF SAMPLE STRUCTURE AND GROWTH

The InGaAs/GaAs sample^{S1-S3} consists of a single layer of nominally InAs quantum dots (QDs) placed within a microcavity structure which is used to select and enhance the photoluminescence from part of the inhomogeneous distribution of QD energies. The sample was grown by molecular beam epitaxy. The QDs were formed by deposition of 1.85 monolayers (MLs) of InAs - just above that required for the nucleation of dots. As a result, we obtain a low density of QDs at the post-nucleation stage. The cavity Q factor is ~ 250 and the cavity has a low temperature resonant wavelength at around 920 nm.

The GaAs/AlGaAs sample investigated contains interface quantum dots (QDs) formed by 1 ML width fluctuations in a thin GaAs quantum well (QW) embedded in an $\text{Al}_{0.3}\text{Ga}_{0.7}\text{As}$ matrix^{S4-S6}. A nominal 9 ML thick GaAs QW layer was embedded between two 50 nm thick barriers. Clear QD signatures appear in the transition region of the sample between regions with QW thicknesses differing by one ML. In the present study, the sample used had QDs with lateral sizes below 30 nm.

Similar to our previous work^{S3,S7-S9}, the InP/GaInP sample was grown in a horizontal flow quartz reactor using low-pressure MOVPE on (100) GaAs substrates misoriented by 3° towards $\langle 111 \rangle$. A low InP growth rate of 1.1 \AA/s and deposition time of 10 seconds were chosen to produce low QD density.

S2. DETAILS OF EXPERIMENTAL TECHNIQUES

The experiments are performed with the sample placed in an exchange-gas cryostat at $T = 4.2 \text{ K}$, and using an external magnetic field B_z normal to the sample surface. We used $B_z \approx 3.2 \text{ T}$ for GaAs/AlGaAs, $B_z \approx 8 \text{ T}$ for InGaAs/GaAs and $B_z \approx 6.3 \text{ T}$ for InP/GaInP samples respectively.

In order to detect nuclear polarization on the dot we use high resolution micro-photoluminescence (μ -PL) spectroscopy of single QDs. The QD PL is excited by a laser resonant with the wetting layer states for self-assembled dots ($E_{exc}=1.46$ eV for InGaAs dots and $E_{exc}=1.88$ eV for InP dots) or tuned above quantum well states for interface GaAs dots ($E_{exc}=1.80$ eV). The PL signal of the neutral quantum dots reported throughout this work is analyzed with a double spectrometer with focal length of 1 meter coupled to a CCD.

Manipulation of nuclear spin polarization relies on the hyperfine interaction of electrons and nuclear spins. Excitation with circularly polarized light generates spin polarized electrons, which transfer spin polarization to nuclear spins via the hyperfine interaction^{S10-S15}. In this work dynamic nuclear polarization of nuclear spins is achieved using high power optical pumping. Optical powers exceeding the QD saturation level (optical power for which neutral exciton PL reaches maximum intensity) by more than a factor of 10 are typically used^{S15}. At these powers the dependence of the steady-state nuclear polarization on the optical power saturates. This ensures (i) large initial degree of nuclear spin polarization as well as (ii) its good stability due to insensitivity to laser power fluctuations. The initial degree of nuclear spin polarization is controlled by changing the degree of the circular polarization of the pump pulse^{S7}. By contrast the laser probe pulse has very small optical power (1/1000 - 1/100 of the saturation power), so that bright and dark excitons have comparable PL intensities^{S15} and both electron and hole hyperfine shifts can be detected simultaneously (see Fig. 1(a) of the main text).

The duration of the pump pulse (4.5÷6.5 s, depending on the type of QDs and magnetic field) is chosen to be long enough to produce the same level of nuclear polarization independent of its initial state before the pump pulse (see timing diagram in Fig. 1 (b) of the main text). The duration of the probe (0.1÷0.5 s) is short enough so that its effect on nuclear spin polarization can be neglected^{S8}. The duration of the radio-frequency (rf) pulse used for isotope selection depends strongly on the QD material: it is ~ 0.15 s for strain-free GaAs QDs and as large as 35 s for strained self-assembled QDs. However in all experiments the total duration of the rf and probe pulses is small compared to the intrinsic nuclear spin decay times^{S5,S8,S16}: the natural depolarization of the isotopes out of resonance is negligible thus ensuring the validity of the isotope selection techniques described below in Sec. S3.

S3. ISOTOPE SELECTIVE DEPolarIZATION OF NUCLEAR SPINS

The electron and hole hyperfine shifts that are used in this work to measure hole hyperfine constants have comparable contributions from different isotopes present in the quantum dot. In order to access hole hyperfine constants of the individual isotopes their hyperfine shifts must be differentiated. As explained in the main text this is achieved by selective depolarization of a chosen isotope using resonant radiofrequency (rf) magnetic field that induces dipole transitions between spin sublevels of the nuclei^{S17}. The rf field perpendicular to the external magnetic field is induced by a mini-coil wound around the sample^{S3,S4,S6}.

The properties of the nuclear spins differ for the quantum dot materials used in this work. In the subsequent subsections we discuss the particular aspects of the experimental techniques for each material system studied.

A. Nuclear magnetic resonance and isotope selection in strain-free GaAs/AlGaAs quantum dots

In order to select the properties of the rf pulse for isotope selective nuclear spin depolarization we first perform nuclear magnetic resonance (NMR) measurements. A typical NMR spectrum of a GaAs/AlGaAs QD^{S18} measured at $B_z \approx 8$ T is shown in Fig. S1 (a). The experiments were performed using optical pump-probe techniques^{S6} with the rf-pulse applied in the dark, and nuclear spin polarization probed by a short optical pulse. Fig. S1 (a) shows the spectral splitting of two bright exciton states as a function of the rf frequency. Resonant depolarization corresponding to all three isotopes of GaAs (^{75}As , ^{69}Ga , ^{71}Ga) is clearly observed. We find no contribution from the ^{27}Al isotope of the quantum well barrier and estimate that the contribution of this isotope to the total Overhauser shift is less than 3% and can be neglected.

In GaAs QDs both gallium isotopes yield resonances with linewidths of 30 kHz, while the arsenic resonance has a linewidth of 100 kHz. The linewidths are mainly determined by quadrupole broadening originating from residual strain, an effect more pronounced for arsenic due to its larger quadrupole moment. In order to achieve quick and almost complete depolarization of a selected isotope we use rf excitation with a rectangular shaped spectral band, 600 kHz wide with the central frequency corresponding to the measured resonance frequency. Within the band, the rf signal has a constant average spectral power density (a white noise type), with the power density outside the bands ~ 1000 smaller than inside the band (to avoid depolarization of other isotopes). The

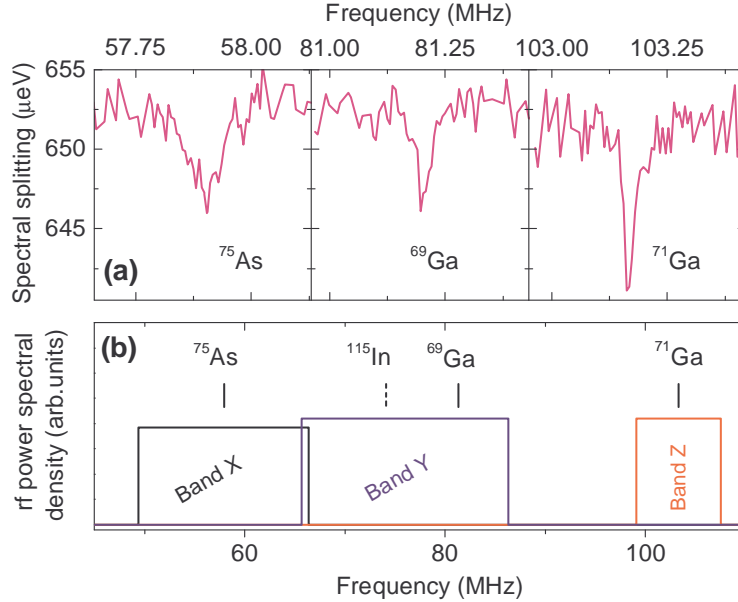


FIG. S1. (a) Optically detected NMR spectrum of a single neutral GaAs QD at $B_z \approx 8.0$ T. Gallium resonances with widths of ~ 30 kHz are observed at ≈ 81.21 MHz and ≈ 103.17 MHz for ^{69}Ga and ^{71}Ga respectively. The arsenic resonance observed at ≈ 57.9 MHz has a linewidth of ~ 100 kHz, which is determined by residual elastic strain. (b) Schematic diagram of the radio-frequency excitation spectrum used to erase nuclear polarization of different isotopes in InGaAs QDs at $B_z \approx 8.0$ T. The solid vertical bars show resonance frequencies of gallium and arsenic derived from (a), while the dashed line shows the calculated central frequency ≈ 74.14 MHz of ^{115}In . Bands X and Z are used to erase nuclear polarization of ^{75}As and ^{71}Ga respectively. Band Y is used to erase polarization of both ^{115}In and ^{69}Ga simultaneously.

duration of the rf pulse (typically 0.15 s) is chosen to be long enough to achieve nearly complete depolarization of the selected isotope. For experiments with depolarization of both gallium isotopes we use an rf signal consisting of two equal spectral bands centered at the corresponding resonant frequencies.

B. Isotope selection in strained InGaAs/GaAs quantum dots

Isotope-selective depolarization of nuclear spins in self-assembled InGaAs/GaAs QDs is more challenging, due to their more complicated nuclear spin system. Significant lattice mismatch results in strain-induced quadrupole shifts^{S13,S15,S19} in these structures. From our recent measurements of the NMR spectra^{S3} we find that such broadening is as large as ~ 10 MHz. Since the rf field couples only spin levels with I_z differing by ± 1 , complete depolarization of the nuclear spin requires that all nuclear spin transitions (corresponding to all I_z) are driven by the rf field *simultaneously*. Because

quadrupole shifts are distributed non-uniformly within the dot, complete depolarization of all nuclei requires an rf field with non-zero components at all frequencies in a broad spectral band. Ideally such a spectrum may be realized by a white noise signal limited in the spectral domain. In experiment we approximate the spectrally limited white noise with rectangular shaped bands that consist of a large number of equally spaced delta-function-like modes. The mode spacing of ≈ 250 Hz is typically used (both for strained and unstrained dots), comparable to the intrinsic linewidth of an individual nuclear spin transition, thus giving a good approximation to white noise (see details in Ref.^{S3}).

Based on NMR spectra measured for InGaAs QDs we choose three different bands of rf excitation shown in Fig. S1 (b). At $B_z = 8$ T bands X and Z are used to erase the polarization of ^{75}As and ^{71}Ga respectively. However, the frequencies of ^{115}In and ^{69}Ga are too close for these isotopes to be addressed individually. For that reason, we use rf excitation with the broad band Y, which erases the polarization of both isotopes [Fig. S1 (b)]. The contributions of ^{115}In and ^{69}Ga can be separated if we assume that both gallium isotopes have the same degrees of spin polarization $\langle I_z^{69\text{Ga}} \rangle = \langle I_z^{71\text{Ga}} \rangle$ as a result of nuclear spin pumping. Such an assumption is justified by the fact that both isotopes have the same spin $I = 3/2$ and both become polarized due to the hyperfine interaction with the optically polarized electrons. Since two gallium isotopes have the same normalized hole hyperfine constants ($\gamma^{69\text{Ga}} = \gamma^{71\text{Ga}}$), we can calculate the Overhauser shifts of ^{69}Ga from the measured shifts of ^{71}Ga (shown in Fig. 2(b) of the main text). For that we need to take into account the ratio of natural abundances of these isotopes, $\rho^{69\text{Ga}}/\rho^{71\text{Ga}} \approx 1.5$, and the ratio of the absolute magnitudes of the electron hyperfine constants, $A^{69\text{Ga}}/A^{71\text{Ga}}$, equal to the ratio of the magnetic moments $\mu^{69\text{Ga}}/\mu^{71\text{Ga}} \approx 0.79$. Thus the electron (hole) hyperfine shifts of indium can be written as $\Delta E_{e(h)}^{\text{In}} = \Delta E_{e(h)}^{\text{In}+^{69}\text{Ga}} - \frac{\rho^{69\text{Ga}}}{\rho^{71\text{Ga}}} \frac{\mu^{69\text{Ga}}}{\mu^{71\text{Ga}}} \Delta E_{e(h)}^{71\text{Ga}}$. This expression is used to estimate the hyperfine constant of indium as described in the main text.

Since the total spectral widths of the rf bands used for experiments on InGaAs QDs are on the order of ~ 10 MHz, the power of the rf field is spread over a large frequency range (the total power is restricted to limit sample heating that does not exceed 1 K in our experiments). As a result erasing nuclear polarization in InGaAs QDs requires long rf pulses (20 \div 35 seconds depending on isotope). This however, is balanced by the long intrinsic nuclear spin decay times (of several hours) observed in strained quantum dots^{S8,S16}: the natural depolarization of the isotopes out of resonance with the rf pulse is negligible within its duration.

C. Isotope selection in strained InP/GaInP quantum dots

The electron hyperfine shift induced by the ^{31}P isotope is very small ($\sim 10 \mu\text{eV}$) due to its small nuclear spin $I=1/2$. This complicates the measurements of the hole hyperfine interaction constant of phosphorus. In order to address this problem we use different isotope selection techniques. Instead of depolarizing phosphorus nuclei we *invert* their polarization thus doubling the electron and hole hyperfine shifts. Such inversion is possible since phosphorus is a spin-1/2 isotope, and is achieved by so called adiabatic rapid passage (ARP) techniques. The concept of ARP is well known^{S20}: the radiofrequency of the oscillating field is "swept" through the resonance. Under appropriate conditions^{S21} such a sweep is adiabatic and nuclear spin polarization along the external field is completely inverted. In our experiments the sweep rate was $\approx 1.5 \text{ MHz/s}$, and the amplitude of the rf field is characterized by a Rabi frequency of $\approx 2 \text{ kHz}$. The rf frequency is swept in the range $\pm 60 \text{ kHz}$ around the ^{31}P resonance frequency (which was $\approx 111.2 \text{ MHz}$); this range significantly exceeds the resonance linewidth ($\approx 8 \text{ kHz}$).

When the phosphorus hyperfine shift is separated (by depolarization or ARP), the remaining hyperfine shifts correspond to the combined effect of indium and gallium. However, in the studied InP/GaInP quantum dots the hyperfine shift due to gallium nuclei is less than 10% of that induced by indium^{S3}. Furthermore using the results for GaAs and InGaAs quantum dots we expect that indium and gallium have hole hyperfine constants of the same sign and of comparable magnitudes. Thus a reasonably accurate value for the normalized hole hyperfine constant of indium in InP dots γ^{In} can be obtained just by subtracting the phosphorus polarization from the total polarization without further manipulations of the gallium polarization.

S4. CALCULATION OF THE VALENCE BAND HYPERFINE INTERACTION STRENGTH

The Hamiltonian for the magnetic interaction of a single electron and a nuclear spin can be written as^{S17,S22–S25}:

$$\hat{\mathcal{H}}_{hf} = 2\mu_B\mu_I\vec{I} \left[\frac{8\pi}{3}\hat{s}\delta(\vec{r}) + \frac{\hat{l}}{r^3} - \frac{\hat{s}}{r^3} + 3\frac{\vec{r}(\hat{s}\cdot\vec{r})}{r^5} \right]. \quad (\text{S1})$$

Here the following notations are introduced: μ_B is the Bohr magneton, μ_I is the nuclear magnetic moment, $\vec{I} = (I_x, I_y, I_z)$ is the nuclear spin, $\hat{l} = -i[\vec{r} \times \vec{\nabla}]$ is the orbital momentum operator of an electron, and \hat{s} is the electron spin operator. It is assumed in Eq. (S1) that the nucleus is

positioned at the origin of coordinates, i.e. at $\vec{r} = 0$. The first term in square brackets in Eq. (S1) describes the Fermi contact interaction of electron and nuclear spins while the last three terms are referred to as the dipole-dipole interaction.

The magnitude of the hyperfine interaction for a particular nucleus is given by the matrix element of the Hamiltonian [Eq. (S1)] calculated using microscopic Bloch wavefunctions. Following the approach of Refs.^{S22–S24} we substitute the electron wavefunction of the crystal with the wavefunction of a single ion. This way we also simplify the calculations of this section by considering only one isotope and omitting additional superscript indices (i.e. we write γ , A instead of γ^k , A^k , etc.). The total hole hyperfine interaction is a sum of contributions from all isotopes.

The wavefunction of an ion can be approximated with hydrogenic eigenfunctions with appropriate effective charges^{S26}. The angular part of each hydrogenic wavefunction is given by a spherical harmonic $Y_{l,m}(\theta, \phi)$ corresponding to a particular orbital momentum l . There is a $(2l + 1)$ -fold degeneracy corresponding to magnetic quantum number m . The symmetry of the crystal imposes restrictions on the wavefunction, partly removing these degeneracies. In order to take this into account in our calculations we select only those combinations of spherical harmonics that transform according to the relevant representation (depending on whether it is conduction or valence band electron) of the point group symmetry of the crystal^{S27}.

The point symmetry of the bulk III-V semiconductor under study (GaAs, InAs, InP) is described by the symmetry group T_d . The relevant spinor representations which describe transformations of the wavefunctions at the Γ point are the two-fold degenerate, Γ_6 , for the conduction band bottom and the four-fold degenerate, Γ_8 , for the valence band top. The basis functions for these representations can be composed as products of the orbital functions and spinors. For the electron in the conduction band we consider the states

$$\begin{aligned}\psi_{\uparrow}(\vec{r}) &= \mathcal{S}(\vec{r})|\uparrow\rangle \\ \psi_{\downarrow}(\vec{r}) &= \mathcal{S}(\vec{r})|\downarrow\rangle,\end{aligned}\tag{S2}$$

where $\mathcal{S}(\vec{r})$ is the orbital function transforming according to the scalar A_1 representation of the T_d point group and $|\uparrow\rangle$, $|\downarrow\rangle$ are spinors corresponding to electron spin projections $\pm 1/2$ onto a quantization axis, which we take as $Oz \parallel [001]$. The valence band at Γ point is constructed of states with Oz momentum projections $\pm 3/2$ (heavy holes) or $\pm 1/2$ (light holes). The wavefunctions are

taken in the form^{S28}:

$$\begin{aligned}
\varphi_{+3/2}(\vec{r}) &= -\frac{\mathcal{X}(\vec{r}) + i\mathcal{Y}(\vec{r})}{\sqrt{2}}|\uparrow\rangle \\
\varphi_{-3/2}(\vec{r}) &= \frac{\mathcal{X}(\vec{r}) - i\mathcal{Y}(\vec{r})}{\sqrt{2}}|\downarrow\rangle \\
\varphi_{+1/2}(\vec{r}) &= -\frac{\mathcal{X}(\vec{r}) + i\mathcal{Y}(\vec{r})}{\sqrt{6}}|\downarrow\rangle + \frac{\sqrt{2}\mathcal{Z}(\vec{r})}{\sqrt{3}}|\uparrow\rangle \\
\varphi_{-1/2}(\vec{r}) &= \frac{\mathcal{X}(\vec{r}) - i\mathcal{Y}(\vec{r})}{\sqrt{6}}|\uparrow\rangle + \frac{\sqrt{2}\mathcal{Z}(\vec{r})}{\sqrt{3}}|\downarrow\rangle.
\end{aligned} \tag{S3}$$

Here the orbital functions $\mathcal{X}(\vec{r})$, $\mathcal{Y}(\vec{r})$ and $\mathcal{Z}(\vec{r})$ form a basis of the three-dimensional representation F_2 of the T_d point symmetry group.

In order to calculate the hyperfine interaction we write orbitals $\mathcal{S}(\vec{r})$, $\mathcal{X}(\vec{r})$, $\mathcal{Y}(\vec{r})$ and $\mathcal{Z}(\vec{r})$ as linear combinations of wavefunctions with defined orbital momentum l and satisfying the symmetry of the corresponding representation (A_1 for $\mathcal{S}(\vec{r})$ and F_2 for $\mathcal{X}(\vec{r})$, $\mathcal{Y}(\vec{r})$, $\mathcal{Z}(\vec{r})$):

$$\begin{aligned}
\mathcal{S}(\vec{r}) &= \mathbb{Y}_{0,0}\mathbb{S}(r) \\
\mathcal{X}(\vec{r}) &= \sum_l \alpha_l X_l(\theta, \phi) R_l(r) \\
\mathcal{Y}(\vec{r}) &= \sum_l \alpha_l Y_l(\theta, \phi) R_l(r) \\
\mathcal{Z}(\vec{r}) &= \sum_l \alpha_l Z_l(\theta, \phi) R_l(r) \\
\sum_l |\alpha_l|^2 &= 1.
\end{aligned} \tag{S4}$$

Here we factored each term into a real radial part $\mathbb{S}(r)$ or $R_l(r)$ and an angular part $X_l(\theta, \phi)$, $Y_l(\theta, \phi)$, $Z_l(\theta, \phi)$ (corresponding to orbital momentum $l > 0$) or $\mathbb{Y}_{0,0} = \frac{1}{2\sqrt{\pi}}$ (corresponding to $l = 0$). The following real linear combinations of spherical harmonics $\mathbb{Y}_{l,m}$ transform according to the F_2 representation^{S27} and correspond to p and d shells ($l=1$ and 2 respectively):

$$\begin{aligned}
X_p(\theta, \phi) &= \frac{1}{\sqrt{2}}[\mathbb{Y}_{1,+1}(\theta, \phi) - \mathbb{Y}_{1,-1}(\theta, \phi)] \\
Y_p(\theta, \phi) &= \frac{-i}{\sqrt{2}}[\mathbb{Y}_{1,+1}(\theta, \phi) + \mathbb{Y}_{1,-1}(\theta, \phi)] \\
Z_p(\theta, \phi) &= \mathbb{Y}_{1,0}(\theta, \phi) \\
X_d(\theta, \phi) &= \frac{i}{\sqrt{2}}[\mathbb{Y}_{2,+1}(\theta, \phi) + \mathbb{Y}_{2,-1}(\theta, \phi)] \\
Y_d(\theta, \phi) &= \frac{-1}{\sqrt{2}}[\mathbb{Y}_{2,+1}(\theta, \phi) - \mathbb{Y}_{2,-1}(\theta, \phi)] \\
Z_d(\theta, \phi) &= \frac{-i}{\sqrt{2}}[\mathbb{Y}_{2,+2}(\theta, \phi) - \mathbb{Y}_{2,-2}(\theta, \phi)]
\end{aligned} \tag{S5}$$

Since the electron orbital wavefunction has s -symmetry only the contact part of the interaction contributes to the Hamiltonian (S1) that can be rewritten as $\hat{\mathcal{H}}_{hf,e} = A(\hat{\mathbf{s}} \cdot \vec{I})$, with conduction band hyperfine constant defined as:

$$A = \langle \psi_{\uparrow}(\vec{r}) | \hat{H}_{hf} | \psi_{\uparrow}(\vec{r}) \rangle / (sI) = -\langle \psi_{\downarrow}(\vec{r}) | \hat{H}_{hf} | \psi_{\downarrow}(\vec{r}) \rangle / (sI) = 2\mu_B\mu_I \left(\frac{8\pi}{3} |\mathcal{S}(0)|^2 \right) = 2\mu_B\mu_I \left(\frac{8\pi}{3} \frac{|\mathcal{S}(0)|^2}{4\pi} \right) = \frac{4}{3} \mu_B\mu_I |\mathcal{S}(0)|^2, \quad (\text{S6})$$

where matrix elements are calculated for nuclear spin aligned along the Oz axis ($I_z = I$).

The hole-nuclear coupling is determined by the dipole-dipole interaction, since the contact term vanishes. The hyperfine interaction of the holes can be obtained by calculating the matrix elements of the Hamiltonian S1 on the valence band states given by Eq. S3. Using Eqns. S4, S5 we obtain the following expression for the hole hyperfine Hamiltonian in the $(\varphi_{+3/2}, \varphi_{+1/2}, \varphi_{-1/2}, \varphi_{-3/2})$ basis:

$$\hat{H}_{hf,h} = \frac{A}{2} \times \begin{pmatrix} (\frac{12}{5}\tilde{M}_p - \frac{18}{7}\tilde{M}_d)I_z & (\frac{4\sqrt{3}}{5}\tilde{M}_p - \frac{9\sqrt{3}}{7}\tilde{M}_d)I_- & 0 & \frac{9}{7}\tilde{M}_dI_+ \\ (\frac{4\sqrt{3}}{5}\tilde{M}_p - \frac{9\sqrt{3}}{7}\tilde{M}_d)I_+ & (\frac{4}{5}\tilde{M}_p - \frac{18}{7}\tilde{M}_d)I_z & (\frac{8}{5}\tilde{M}_p - \frac{9}{7}\tilde{M}_d)I_- & 0 \\ 0 & (\frac{8}{5}\tilde{M}_p - \frac{9}{7}\tilde{M}_d)I_+ & (-\frac{4}{5}\tilde{M}_p + \frac{18}{7}\tilde{M}_d)I_z & (\frac{4\sqrt{3}}{5}\tilde{M}_p - \frac{9\sqrt{3}}{7}\tilde{M}_d)I_- \\ \frac{9}{7}\tilde{M}_dI_- & 0 & (\frac{4\sqrt{3}}{5}\tilde{M}_p - \frac{9\sqrt{3}}{7}\tilde{M}_d)I_+ & (-\frac{12}{5}\tilde{M}_p + \frac{18}{7}\tilde{M}_d)I_z \end{pmatrix},$$

$$\tilde{M}_l = |\alpha_l|^2 M_l, \quad l = p, d,$$

$$M_l = \frac{1}{|\mathcal{S}(0)|^2} \int_0^\infty \frac{R_l^2(r)}{r} dr, \quad l = p, d, \quad (\text{S7})$$

where $I_{\pm} = I_x \pm iI_y$, A is electron hyperfine constant defined in Eq. S6, and radial integrals M_l are always positive. Also we restrict our analysis to two shells (p and d), so that $|\alpha_p|^2 + |\alpha_d|^2 = 1$.

The Hamiltonian S7 can also be rewritten in the following form:

$$\hat{H}_{hf,h} = \frac{A}{2} \left[\left(\frac{8}{5}\tilde{M}_p - \frac{39}{7}\tilde{M}_d \right) (\hat{J}_x I_x + \hat{J}_y I_y + \hat{J}_z I_z) + \frac{12}{7}\tilde{M}_d (\hat{J}_x^3 I_x + \hat{J}_y^3 I_y + \hat{J}_z^3 I_z) \right], \quad (\text{S8})$$

where $\hat{J}_x, \hat{J}_y, \hat{J}_z$ are the components of the $J = 3/2$ hole total momentum operator. The first term in Eq. S8 (proportional to the first power of \hat{J}) is a spherical invariant and contains contributions from both p and d shells. By contrast the second term (proportional to the third power of \hat{J}) has lower symmetry corresponding to the cubic T_d point group. This term is completely determined by the contribution of the d shells.

The hole hyperfine constant C is defined similarly to the electron hyperfine constant. Also, such definition is equivalent to that of the main text (see Eqs. 1, 2 of the main text):

$$C = \langle \varphi_{+3/2} | \hat{H}_{hf} | \varphi_{+3/2} \rangle / (sI) = -\langle \varphi_{-3/2} | \hat{H}_{hf} | \varphi_{-3/2} \rangle / (sI), \quad (\text{S9})$$

where $s = 1/2$, nuclear spin is aligned along Oz axis ($I_z = I$) and we assume by definition that the hole wavefunctions correspond to the heavy hole states (denoted as \uparrow , \downarrow in the main text). According to Eq. S9 the normalized heavy hole hyperfine constant $\gamma = C/A$ (measured experimentally) is given by the expression in the brackets in the first diagonal element of the hyperfine Hamiltonian S7:

$$\gamma = \frac{a_v}{a_c} \left(\frac{12}{5} |\alpha_p|^2 M_p - \frac{18}{7} |\alpha_d|^2 M_d \right). \quad (\text{S10})$$

Here we introduced a renormalization factor which takes into account the fact that the contribution of the atomic shells into the valence band a_v and into the conduction band a_c depend on the isotope. The calculated values of a_v and a_c reported in the literature differ depending on the model used^{S29}. For example Boguslawski *et al.*^{S30} found $a_v = 35\%$, $a_c = 49\%$ for gallium and $a_v = 65\%$, $a_c = 51\%$ for arsenic in GaAs, which means that the value of γ in the crystal differs from that calculated for isolated ions by $\sim 30\div 40\%$. However such corrections do not affect the main conclusion that can be drawn from Eq. S10: regardless of the actual values of a_v and a_c and the actual expression for $R_l(r)$, p -symmetry states give a positive contribution to γ , while for the d -shell it is negative. For simplicity, in what follows and in the analysis of the main text we neglect the difference in the contribution of cations and anions to the conduction and valence bands by setting a_v and a_c to 50% for all isotopes.

When dealing with the valence band states it is important to bear in mind a distinction between electron and hole representations. Hamiltonian S1 is written in the electron representation, i.e. it corresponds to the energies of *filled* valence band states. When switching to the hole representation, all energies must be taken with a "–" sign since the hole hyperfine energy is the energy of an electron *removed* from the valence band. On the other hand spin and orbital momenta also have opposite signs in electron and hole representations. By definition the hole hyperfine constant γ is proportional to the energy splitting between the hole "spin up" state and "spin down" state. When switching from electron to hole representation both energy splitting and momenta are inverted. Due to this double inversion the expression for the hole hyperfine constant γ (Eq. S10) remains the same (has the same sign) in both representations. This expression also coincides with the definition used in the main text when describing the experimental results. Care should be taken when considering the sign of γ , since there has been some disagreement in recent publications: Ref.^{S22} predicted positive γ for p -symmetry holes in agreement with the above discussion, while Ref.^{S23} predicted negative γ .

In order to obtain numerical estimates of the heavy hole hyperfine interaction strength in

TABLE S1. Orbital exponents, ξ for Ga and As. Data taken from Ref.^{S26}.

	$\xi(4s)$	$\xi(3d)$	$\xi(4p)$
Ga	1.7667	5.0311	1.554
As	2.2360	5.7928	1.8623

GaAs (see main text) we approximate the wavefunctions in Eq. S10 with hydrogenic orbitals. In particular the conduction band state $\mathcal{S}(\vec{r})$ is approximated with the 4s hydrogen function, while for valence band holes we include the contribution of 4p and 3d shells. Wavefunctions that take into account electron-electron interactions are obtained from standard radial hydrogenic functions \mathcal{R}_{nl} by replacing the ion charge Z with an effective charge^{S23} $Z_{eff} = n\xi(n, l)$, where n is the principle quantum number of the shell and $\xi(n, l)$ is the orbital exponent^{S26} given in Table. S1. The values of $\xi(n, l)$ are different for particular shells and isotopes resulting in variation of the calculated hyperfine integrals, which are $M_p = 0.05687$, $M_d = 0.3849$ for gallium and $M_p = 0.04815$, $M_d = 0.2898$ for arsenic.

S5. HOLE HYPERFINE INTERACTION IN QUANTUM DOTS

In III-V semiconductor quantum dots heavy and light holes are well separated in energy by the heavy-light splitting, which exceeds ~ 10 meV. Thus hyperfine effects can be considered as a perturbation and we can introduce 1/2 pseudospin operators \hat{S}^{hh} and \hat{S}^{lh} with z -projections $\pm 1/2$ corresponding to the hole momentum z -projection $\pm 3/2$ (for heavy hole subspace) or $\pm 1/2$ (for light hole subspace). Using Eq. S7 the hyperfine Hamiltonians for hh and lh doublets can be written as:

$$\begin{aligned} \hat{\mathcal{H}}_{hf}^{hh} &= \sum_j \frac{A^j}{2} |\Psi_{\pm 3/2}(\vec{R}_j)|^2 \left[\left(\frac{12}{5} \tilde{M}_p - \frac{18}{7} \tilde{M}_d \right) I_z^j \hat{S}_z^{hh} + \frac{9}{7} \tilde{M}_d \left(I_x^j \hat{S}_x^{hh} - I_y^j \hat{S}_y^{hh} \right) \right], \\ \hat{\mathcal{H}}_{hf}^{lh} &= \sum_j \frac{A^j}{2} |\Psi_{\pm 1/2}(\vec{R}_j)|^2 \left[\left(\frac{4}{5} \tilde{M}_p - \frac{18}{7} \tilde{M}_d \right) I_z^j \hat{S}_z^{lh} + \left(\frac{8}{5} \tilde{M}_p - \frac{9}{7} \tilde{M}_d \right) \left(I_x^j \hat{S}_x^{hh} + I_y^j \hat{S}_y^{hh} \right) \right], \end{aligned} \quad (\text{S11})$$

where the summation goes over all nuclei j with nuclear spin I^j located at position R_j and $\Psi_{\pm 3/2}$ ($\Psi_{\pm 1/2}$) is a heavy hole (light hole) envelope wavefunction. Eq. S11 extends the expression for the hole hyperfine Hamiltonian derived in Ref.^{S22} for pure p -shell holes.

It follows from Eq. S11 that the hyperfine interaction is anisotropic and has a non-Ising form for both heavy and light holes even in the absence of heavy-light hole mixing. In particular, it can be seen that the flip-flops between the heavy hole states, described by the term proportional to

$(I_x^j \hat{S}_x^{hh} - I_y^j \hat{S}_y^{hh})$ in $\hat{\mathcal{H}}_{hf}^{hh}$ become possible due to the non-zero contribution from the d -shell orbitals ($\tilde{M}_d > 0$). We note that this effect is absent if only s and p -shells are taken into account, since such simplification artificially lifts the overall symmetry of the system to spherical. By contrast the cubic symmetry of the crystal (described by T_d group) can be reproduced correctly only when the d -shells are taken into account.

It has been shown that hole-nuclear spin flips contribute significantly to the spin dephasing of the heavy holes localized in a quantum dot^{S22,S23}. However, previously such flip-flops were attributed solely to the effect of mixing with the light holes for which in-plane hyperfine interaction [proportional to $(I_x^j \hat{S}_x^{lh} + I_y^j \hat{S}_y^{lh})$ in $\hat{\mathcal{H}}_{hf}^{lh}$] exists even at $\tilde{M}_d = 0$. Thus the significant contribution of d -symmetry orbitals reported in this work may be a source of hole spin decoherence due to non-Ising hyperfine interaction even in quantum dots with negligible heavy-light hole mixing.

In order to establish the relative role of the the d -symmetry contribution in hole spin decoherence we estimate the magnitude of the hyperfine interaction with the in-plane nuclear polarization (described by the term in Hamiltonian proportional to $I_x \hat{S}_x$) in two cases (i) pure heavy holes with non-zero d -shell contribution and (ii) mixed heavy-light hole states composed of pure p -shells. In case (i) spin flips are determined by the term $\propto \frac{9}{7} |\alpha_d|^2 M_d I_x \hat{S}_x^{hh}$ of the heavy hole Hamiltonian in Eq. S11. The effect of heavy light hole mixing (ii) has been studied in Ref.S22. In the simplest case of mixing induced by strain the resulting hole states have the form $\tilde{\varphi}_{+3/2} \approx \varphi_{+3/2} + \beta \varphi_{-1/2}$ and $\tilde{\varphi}_{-3/2} \approx \varphi_{-3/2} + \beta^* \varphi_{+1/2}$ where $\beta \ll 1$. The in-plane hyperfine interaction can be derived by calculating the nondiagonal elements of the Hamiltonian Eq. S7 for the $\tilde{\varphi}_{\pm 3/2}$ wavefunctions. The resulting interaction is described by the term $\propto \frac{2|\beta|}{\sqrt{3}} \frac{12}{5} M_p I_x \hat{S}_x$ (this result coincides with Eq. 17 of Ref.S22). In order to obtain numerical estimates we use the calculated values of M_p and M_d for gallium and also take the estimate $|\alpha_d|^2 \approx 0.2$ derived in the main text. In this way we find the following values of the non-diagonal matrix elements: $\propto 0.1 I_x \hat{S}_x^{hh}$ for pure heavy holes [case (i)], and $\propto 0.16 |\beta| I_x \hat{S}_x$ for mixed states [case (ii)]. For gallium nuclei these two contributions to the hole-nuclear spin-flips become comparable only at rather large values of the mixing parameter $\beta \sim 0.65$ (corresponding to valence band states with $\sim 30\%$ light hole contribution). Thus under realistic conditions the effect of the cationic d -shells is at least comparable to that of the heavy-light hole mixing and may be a dominant mechanism of the hole spin dephasing (in particular at small β).

It also follows from Eq. S11 that the effective hyperfine constant (along the Oz direction) is different for heavy and light holes. The measured values of γ^k (presented in Table I of the main text) describe the hyperfine interaction of the valence band states that are in general mixed states

of heavy and light holes. Using Eq. S7 we calculate the hole hyperfine constant for $\tilde{\varphi}_{\pm 3/2}$ states to first order in $|\beta|^2$:

$$\begin{aligned} \tilde{\gamma}^k = \left(\frac{12}{5}|\alpha_p|^2 M_p - \frac{18}{7}|\alpha_d|^2 M_d \right) - \frac{4}{3}|\beta|^2 \left(\frac{12}{5}|\alpha_p|^2 M_p - \frac{27}{7}|\alpha_d|^2 M_d \right) = \\ \gamma^k - \frac{4}{3}|\beta|^2 \left(\frac{12}{5}|\alpha_p|^2 M_p - \frac{27}{7}|\alpha_d|^2 M_d \right). \end{aligned} \quad (\text{S12})$$

In quantum dots with mixed heavy and light holes it is the value of $\tilde{\gamma}^k$ that is measured experimentally.

An upper limit for the contribution of light holes can be estimated from the measured degree of circular polarization σ_c (where $-1 \leq \sigma_c \leq 1$) of the bright exciton luminescence^{S7}. The emission of the $\uparrow\downarrow$ bright exciton is predominantly σ^+ polarized ($\sigma_c > 0$), while it is mainly σ^- polarized for $\downarrow\uparrow$ ($\sigma_c < 0$). Using the matrix elements for the dipole transitions of the light and heavy holes^{S28} we can calculate the polarization degree of the exciton luminescence:

$$|\sigma_c| = (1 - |\beta|^2/3)/(1 + |\beta|^2/3), \quad (\text{S13})$$

with the ideal value of $|\sigma_c| = 1$ corresponding to pure heavy hole states.

It follows from Eq. S12 that $\tilde{\gamma}^k$ is not proportional to γ^k , i.e. the effect of the heavy-light hole mixing depends on the actual orbital composition of the wavefunction (on $|\alpha_p|^2$ and $|\alpha_d|^2$). In order to obtain numerical estimates for the changes in γ^k due to the heavy-light hole mixing we consider GaAs. From the results of the main text we take the calculated values for M_p and M_d and $|\alpha_d|^2 \approx 0.2$ for gallium and $|\alpha_d|^2 \approx 0$ for arsenic ($|\alpha_p|^2 = 1 - |\alpha_d|^2$). Using Eqs. S12, S13 we obtain the following estimates (to first order in $1 - |\sigma_c|$) for the heavy hole hyperfine constant γ^k expressed in terms of the measured $\tilde{\gamma}^k$ corresponding to the mixed holes states:

$$\begin{aligned} \gamma^{Ga} &\approx \tilde{\gamma}^{Ga} - 0.38(1 - |\sigma_c|), \\ \gamma^{As} &\approx \tilde{\gamma}^{As} + 0.23(1 - |\sigma_c|). \end{aligned} \quad (\text{S14})$$

According to Eq. S14 the actual value of γ^k is larger in absolute value than $\tilde{\gamma}^k$ for both gallium and arsenic. Thus heavy-light hole mixing can be excluded in playing a role in determining the opposite signs of γ^k for cations and anions, the main experimental observation of this work.

In the studied GaAs quantum dots $|\sigma_c| \sim 85 \div 95\%$ is observed. Using Eq. S14 we find that the maximum possible correction due to heavy-light hole mixing is $\gamma^{Ga} - \tilde{\gamma}^{Ga} \approx -0.056$ for gallium and $\gamma^{As} - \tilde{\gamma}^{As} \approx +0.035$ for arsenic. Much higher degree of circular polarization $|\sigma_c| > 95\%$ is found for InGaAs dots, and corrections to γ^k are even smaller. In InP dots somewhat smaller

degree of circular polarization $|\sigma_c| \sim 80 \div 90\%$ is observed. This agrees with the increased dot-to-dot variation of γ^{In} (see Table I of the main text). We note that the estimates based on the measurement of σ_c give an upper limit to the possible correction of γ^k due to heavy-light hole mixing, since reduced circular polarization degree $|\sigma_c| < 1$ can be a result of other factors such as non-ideal polarization optics. In particular, this is likely to be the case for nearly strain-free GaAs dots where heavy-light hole mixing is expected to be very small.

We also find that the systematic errors in measurements of γ^k , such as fine structure splitting of bright exciton and mixing between bright and dark excitons are negligible in the studied structures (the details of such estimates were reported previously in Ref.^{S7}).

-
- S1. Daraei, A. *et al.* Control of polarized single quantum dot emission in high-quality-factor microcavity pillars. *Appl. Phys. Lett.* **88**, 051113 (2006).
 - S2. Sanvitto, D. *et al.* Observation of ultrahigh quality factor in a semiconductor microcavity. *Appl. Phys. Lett.* **86**, 191109 (2005).
 - S3. Chekhovich, E. A., *et al.* Structural analysis of strained quantum dots using nuclear magnetic resonance. *Nature Nanotech.* DOI:10.1038/NNANO.2012.142 (2012).
 - S4. Makhonin, M. N. *et al.* Optically tunable nuclear magnetic resonance in a single quantum dot. *Phys. Rev. B* **82**, 161309 (2010).
 - S5. Nikolaenko, A. E. *et al.* Suppression of nuclear spin diffusion at a GaAs/Al_xGa_{1-x}As interface measured with a single quantum-dot nanoprobe. *Phys. Rev. B* **79**, 081303 (2009).
 - S6. Makhonin, M. N. *et al.* Fast control of nuclear spin polarization in an optically pumped single quantum dot. *Nature Materials* **10**, 844–848 (2011).
 - S7. Chekhovich, E. A., Krysa, A. B., Skolnick, M. S., and Tartakovskii, A. I. Direct measurement of the hole-nuclear spin interaction in single InP/GaInP quantum dots using photoluminescence spectroscopy. *Phys. Rev. Lett.* **106**, 027402 (2011).
 - S8. Chekhovich, E. A. *et al.* Dynamics of optically induced nuclear spin polarization in individual InP/Ga_xIn_{1-x}P quantum dots. *Phys. Rev. B* **81**, 245308 (2010).
 - S9. Chekhovich, E. A. *et al.* Pumping of nuclear spins by optical excitation of spin-forbidden transitions in a quantum dot. *Phys. Rev. Lett.* **104**, 066804 (2010).
 - S10. Gammon, D. *et al.* Electron and nuclear spin interactions in the optical spectra of single GaAs quantum dots. *Phys. Rev. Lett.* **86**, 5176–5179 (2001).
 - S11. Tartakovskii, A. I. *et al.* Nuclear spin switch in semiconductor quantum dots. *Phys. Rev. Lett.* **98**, 026806 (2007).
 - S12. Lai, C. W., Maletinsky, P., Badolato, A., and Imamoglu, A. Knight-field-enabled nuclear spin polar-

- ization in single quantum dots. *Phys. Rev. Lett.* **96**, 167403 (2006).
- S13. Eble, B. *et al.* Dynamic nuclear polarization of a single charge-tunable InAs/GaAs quantum dot. *Phys. Rev. B* **74**, 081306 (2006).
- S14. Braun, P.-F. *et al.* Bistability of the nuclear polarization created through optical pumping in $\text{In}_{1-x}\text{Ga}_x\text{As}$ quantum dots. *Phys. Rev. B* **74**, 245306 (2006).
- S15. Chekhovich, E. A., Krysa, A. B., Skolnick, M. S., and Tartakovskii, A. I. Light-polarization-independent nuclear spin alignment in a quantum dot. *Phys. Rev. B* **83**, 125318 (2011).
- S16. Latta, C., Srivastava, A., and Imamoğlu, A. Hyperfine interaction-dominated dynamics of nuclear spins in self-assembled InGaAs quantum dots. *Phys. Rev. Lett.* **107**, 167401 (2011).
- S17. Abragam, A. *The principles of Nuclear Magnetism*. Oxford University Press, London (1961).
- S18. Gammon, D. *et al.* Nuclear Spectroscopy in Single Quantum Dots: Nanoscopic Raman Scattering and Nuclear Magnetic Resonance. *Science* **277**, 85–88 (1997).
- S19. Flisinski, K. *et al.* Optically detected magnetic resonance at the quadrupole-split nuclear states in (In,Ga)As/GaAs quantum dots. *Phys. Rev. B* **82**, 081308 (2010).
- S20. Bloch, F., Hansen, W. W., and Packard, M. The nuclear induction experiment. *Phys. Rev.* **70**, 474–485 (1946).
- S21. Janzen, W. Adiabatic rapid passage NMR signal shape and passage conditions in solids. *Journal of Magnetic Resonance* **12**, 71 – 78 (1973).
- S22. Testelin, C., Bernardot, F., Eble, B., and Chamarro, M. Hole–spin dephasing time associated with hyperfine interaction in quantum dots. *Phys. Rev. B* **79**, 195440 (2009).
- S23. Fischer, J., Coish, W. A., Bulaev, D. V., and Loss, D. Spin decoherence of a heavy hole coupled to nuclear spins in a quantum dot. *Phys. Rev. B* **78**, 155329 (2008).
- S24. Gryncharova, E. I. and Perel, V. I. Relaxation of nuclear spins interacting with holes in semiconductors. *Sov. Phys. Semicond.* **11**, 997 (1977).
- S25. Van de Walle, C. G. and Blöchl, P. E. First-principles calculations of hyperfine parameters. *Phys. Rev. B* **47**, 4244–4255 (1993).
- S26. Clementi, E. and Raimondi, D. L. Atomic screening constants from scf functions. *The Journal of Chemical Physics* **38**, 2686–2689 (1963).
- S27. Altmann, S. L. On the symmetries of spherical harmonics. *Proc. Cambridge Phil. Soc.* **53**, 343 (1956).
- S28. Meier, F. and Zakharchenya, B. P. *Optical Orientation*. Elsevier, New York, (1984).
- S29. Díaz, J. G. and Bryant, G. W. Electronic and optical fine structure of GaAs nanocrystals: The role of d orbitals in a tight-binding approach. *Phys. Rev. B* **73**, 075329 (2006).
- S30. Boguslawski, P. and Gorczyca, I. Atomic-orbital interpretation of electronic structure of III-V semiconductors: GaAs versus AlAs. *Semiconductor Science and Technology* **9**, 2169 (1994).